

Growth inhibition and apoptosis induction in two types of women cancer cell lines using laser ablated silver nanoparticles in polyvinylpyrrolidone solution

Nawfal N. R. ALrawi¹, Mohammed Q. Al-Ani¹, Amer T. Tawfeeq², Nahi Yousif Yaseen²

¹ College of Science-Biology/ University of Anbar

² Iraqi centre for cancer and medical genetics research/ al-Mustansiriya University

Abstract:

Silver nanoparticles (AgNPs) coated with polyvinylpyrrolidone (PVP) was prepared by pulsed laser ablation method in PVP solution, 1000 pulse was used with laser energy of 800 mJ/pulse. Formation of AgNPs-PVP was confirmed by UV-visible spectrophotometer detecting surface plasmon resonance change in the ablation solution. Concentration of AgNPs, size distribution, and surface charge of the ablated AgNPs in the produced solution was determined using atomic absorption spectroscopy and zeta potential analysis respectively. Nanoparticles shape was determined using transmission electron microscope imaging. Ability of the synthesized AgNPs to inhibit the growth of cancer cells was compared to that of normal fibroblast cells using two cancer cell lines (HeLa and SKOV-3) in different concentrations (0.78, 1.56, 3.125, 6.25, 12.5 and 25 µg/ml). The apoptosis events were also detected in both types of cancer cell lines using mitochondrial membrane permeability, nuclear morphology, and genomic DNA fragmentation. The contribution of AgNPs to the levels of glutathione s-transferase was also determined. According to the results, AgNPs size was 28.43nm with spherical shape and peak UV-Vis absorbance ranged between 402-410nm. Concentration of AgNPs in ablated solution was 50 µg/ml and used as stock concentration in cell lines experiments. Ablated silver nanoparticles was capable of inhibit the growth of both HeLa and SKOV-3 cancer cell lines in dose and time dependent manner, whereas it was less inhibitory against normal fibroblast cells. All three apoptosis detection method conducted indicated positive characteristics for apoptosis, while GSH levels did not varied significantly in both HeLa and SKOV-3 cells.

Keywords: AgNPs, cancer cells, metal silver, Cytotoxicity, MTP, DNA fragmentation, GSH.

Introduction:

Cancer is a diseases characterized by abnormal uncontrolled proliferation of cells in a certain tissue. These uncontrolled proliferated cells may gain the ability to transfer to other tissues and establish growth, this spread of abnormal cells called metastases which is the most fatal event in cancer (1, 2). In Iraq, the latest Iraqi Cancer Registry revealed that among an estimated population size of 32,500,000, a total number of 21,101 new cases of cancer were registered in 2012. Collectively 9,268 were in men and 11,833 were women (3, 4). The current medicinal methods to treat cancer include the classical therapeutic procedures such as surgery, chemotherapy, radiation, and hormone therapy. More advanced therapies are in use known such as immunotherapy and targeted therapy (5, 6). These therapies must be aimed to diminish and destroy

only the cancer cells in the tumor mass without affecting the normal cells. But unfortunately these therapeutics have many side effects comes up as a result of effecting normal cells in the normal tissues (7). Nanotechnology is the most promising field for its generating new applications in medicine (8, 9). The term nanotechnology deals with materials ranging in size from 1 to 100 nm. The advancement in the field of nanotechnology and its applications to the field of medicine, pharmaceuticals and biology has revolutionized the twenty-first century (10, 11). In this respect, nanoparticles have received considerable attention in recent years due to their capacity to be introduced in a wide range of applications. In the biomedical sciences, the field has been revolutionized since nanoparticles was used to improve specific biological processes such as gene or agent carriers, and in drug design to improve efficacy and disease treatment or therapeutics modification. They used in labeling of fluorescent agents, tissue engineering, diagnostics, biomarkers, cell labeling, as antimicrobial agents, drug delivery, cancer therapy, and mosquito control (12, 13). One of such nanopar-

Corresponding Address:

Nawfal N. R. ALrawi

College of Science-Biology/ University of Anbar

Email: nwfal85@Gmail.com

articles types that gained attention for its possible application in biology in early stage of this science development was silver nanoparticles (14). Silver nanoparticles have their antimicrobial activities (15), and many of studies used human cancer cells as a model to investigate these particles cytotoxicity (16, 17). Pulse laser ablation in liquid (PLAL) is one of the useful physical techniques to produce nano-materials, such as gold nanoparticles (18), Zinc oxide nanoparticles (19) and silver nanoparticle (20). Moreover, it is also a promising, as a kind of 'green' process with little pollution for the environment. Comparing to chemical methods that increase the risks of using hazardous chemicals and/or releasing harmful byproducts to the environment, PLAL is less stern (21). The visibility to use AgNPs for cancer treatment is an ongoing research task and different scenarios were proposed to meet these requirements (22, 23). Therefore, this study was designed to explore the anticancer activities of physically synthesized AgNPs-PVP using laser device by pulse ablation. Afterword to evaluate its potential anticancer and toxic activity in vitro employing HeLa, SKOV-3 and REF cell lines. The results of present study provide new approaches for treating cervical and ovarian cancers by using silver-based nanoparticle therapies.

Materials and methods:

Culture media preparation

RPMI 1064 culture media with 2 mM L-glutamine and HEPES (USbiological, USA) were prepared, 100 µg/mL penicillin/streptomycin and 10% fetal bovine serum (USbiological, USA) was added. This media was use to maintain ,cultivate the cells, and to carry out the testes.

PVP solutions

Polyvinylpyrrolidone (PVP) K30 solution was prepared by adding (0.05g) of pure PVP powder to 20 ml of deionized distilled water (DDW) with stirring for 30 minute (24) to prepared PVP solution.

Synthesis of silver nanoparticles

To synthesis silver nanoparticles, a Q-switched Nd-YAG laser (type HUAFEI) operating at 1064 nm wavelength was employed. After laser-based setup was constructed, silver particles from metallic silver plate (99.999% purity) immersed in Polyvinylpyrrolidone (PVP) solution was ablated. The plate target was placed at the bottom of a glass cell containing 5ml PVP solution volume and was rotated to avoid deep ablation. The number of pulses utilized to produce the silver nanoparticle solution was 1000 pulses, at laser energy shoot of 800 mJ/pulse. Lasers pulse duration and repetition rate were 10 ns and 10 Hz respectively. The distance between target plate and laser source was 10 cm, diameter of laser spot on a targeted plate was 1mm. After ablation process, a yellowish colloidal solution of silver nanomaterial was obtained.

Characterization of silver nanoparticles

UV-Vis absorbance spectroscopy analysis

Absorbance spectra of the silver nanoparticle solutions were measured by UV-visible spectrophotometer (Metertech SP-8001-Tiwan) directly after synthesis (25). Absorbance spec-

trum was measured at regular different time intervals (after 1 and 2 weeks) to same sample to authenticate the formation and stability of AgNPs-PVP solution.

The zeta potential measurement

The zeta potential measurement was carried out using zetaplus analysis (brookhaven-Milton Keynes, UK). Zeta potential analysis is important to measure the surface charge of silver nanoparticles.

Concentration measurement

Concentration of the synthesized silver nanoparticles was determined using atomic absorption spectroscopy (model Nov AA350, Germany).

Transmission electron microscope analysis (TEM)

Transmission electron microscopy (model CM10 pw6020, Philips-Germany) was used to determine the morphology, size and particle distributions of synthesized AgNPs-PVP. TEM samples were prepared by placing a drop of the suspension of silver nanoparticles solution on grids and allowing its dissolving water to evaporate then been introduced to TEM chamber.

Cell lines

A human cervical cancer cell line, HeLa, and human ovarian cancer cell line, SKOV-3, with an immortal non-cancerous rat embryo fibroblast cell line, REF, were employed in this study, kindly provided by Iraqi Center for Cancer and Medical Genetic Research (ICCMGR). This cell lines were maintained in RPMI-1064 medium with 10% fetal calf serum in a humidified atmosphere and 5 % CO₂ at 37 °C.

Cell viability assay

The cell viability assay was measured using the crystal violet stain which performed to determine the cytotoxic effect of the AgNPs-PVP (at laser energy 800mJ/pulse) at six concentrations (0.78, 1.56, 3.125, 6.25, 12.5 and 25µg/ml). Briefly, the three types of the cells were seeded independently onto 96-well flat bottom culture plates at a density of 1×10^4 cells/well and incubated for 24 hrs. The cells were exposed to prepared concentrations of AgNPs, in addition to control untreated cells. Than all cultures were incubated for 24, 48 and 72hrs at 37°C in a humidified incubator. At the end of the incubation period, the plates were decanted to remove the exposure medium; the wells were washed with 100 µl of PBS. Finally, 50µL of crystal violat stain was added to each well. The plates were incubated for a 20min at 37°C in dark. After that the plates were decanted. The absorbance was measured at 492 nm with a microplate reader (FLUOstar OPTIMA - Germany). The results were given as the mean of three independent experiments. Viability was determined by the following equation: % cell viability = OD of control cells - OD of treated cells/ OD of control cells × 100. The 50% reduction in cell viability (IC₅₀ values) was determined and employed for next tests.

Mitochondrial transmembrane potential assay

Mitochondrion BioAssay Kit (US.Biological) was employed to determine the early events of apoptosis, the treated and control cells was stained with fluorescent dyes. Cells were grown in 96-well flat bottom plates (1×10^4 cells/well), and incubated for 24hrs at 37°C with 5% CO₂. Cells were exposure to AgNPs-PVP IC₅₀ and re-incubated for 24hr. At the end of the in-

incubation time, the exposure media was aspirated. The diluted MitoCapture reagent was added (50µl/well), and plates were covered and incubated for 15min. after incubation the cells were washed twice with buffer solution and observed under an inverted fluorescence microscope (Leica Switzerland) with the blue filters; the microphotographs for cells were obtained with a Leica inverted fluorescent microscope DMI6000 digital camera.

Nuclear morphology assay

In order to confirm the event of apoptosis, the treated and control cells was stained with fluorescent dyes to determine the cells morphology and nucleus shape. Cells were grown in 96-well flat bottom plates (1×10⁴ cells/well), and incubated for 24hrs at 37°C with 5% CO₂. Cells were exposed to IC₅₀ value of the AgNPs in serum free media and re-incubated. After the time of incubation was over media was discarded, Acridine orange and Propidium Iodide (AO/PI) stain mixture (5µg/ml, 10µl) was added over the cells and cover slip was laid. Cells were observed and microphotographs for cells were obtained with a Leica inverted fluorescent microscope DMI6000 digital camera with the blue and green filters.

DNA fragmentation assay

Cells were grown (1x10⁶ cells) in flask 25cm³ in the suitable media for 24 hrs incubation. After those cells were exposed to IC₅₀ value of silver nanoparticles for 24 hrs. Cells were harvested with scraping. MagCore® Genomic DNA Large Volume kit is designed to extract genomic DNA from sample via Magnesia 16 System auto-extraction instrument. The extracted DNA was mixed with DNA loading dye, and then applied to 1% agarose gel electrophoresis. After staining with ethidium bromide (USBiological, USA), the DNA was visualized by UV irradiation and photographed by gel documentation system (Scie-Plus, UK). Molecular weight marker ladder was used to characterize the DNA fragmentation.

Reduced glutathione (GSH) assay

The cells were grown in flask 25cm³ at (1x10⁶ cells) incubation for 24 hrs. Cells were exposed to IC₅₀ value of silver nanoparticles for 24 hrs, without control cells exposure. The cells with supernatant were collected in sterile tube and subject to freeze-thaw cycles to break the cell membranes. Done

centrifuge for tubes at (5000rpm) for 15 min. at 20°C. The supernatant was transfer to new tubes (samples). Samples and standard were incubated together with GSH-HRP conjugate for one hour. A competition for limited antibody binding sites on the plate occur between GSH-HRP conjugate and GSH in the samples and standards. After the incubation, the wells are washed five times with buffer. The wells were incubated with substrate for HRP enzyme. Finally, a stop solution was added to terminate the reaction which will then turn the solution yellow. The intensity of color was measured spectrophotometrically at 450nm in a microplate reader (FLUOstar OPTIMA). A standard curve was plotted relating the intensity of the color (O.D.) to the standard concentrations. The GSH concentration in each sample is interpolated from this standard curve.

Statistical analysis

The Statistical Analysis System-SAS (26) program was used to identify the effect of each factor in the study parameters. Least significant difference–LSD test was used to determined significance between means in this study.

Results and Discussion:

Synthesis and characterization of Ag nanoparticles

Observed change color solutions from colorless and transparent form to slightly yellowish after a few minutes during the ablation of the silver piece (27), Fig-1. Tables-1 shows the types of prepared silver nanoparticles in Polyvinaylpayrolidone (PVP) solution, the laser energy used, the number of laser pulses and the stock concentration (µg/ml).

This was also confirmed by using UV-Vis spectroscopy that shows absorption spectrum for two types of Ag nanoparticles, to know the formation of AgNPs. The UV–Vis spectrometric readings were recorded at a scanning speed of 200 to 1000 nm. The peak ranged at 402-410nm of AgNPs-PVP were the signatures of plasmon peak of AgNPs during 2weeks (table -1), which confirmed the formation of AgNPs, which showed an increased in the formation efficiency of the NPs and indicates a reduction of particle size following the Mie theory (28). Fig-1.

Table-1: types of nanoparticles synthesis by laser ablation technique with it stock concentration.

AgNPs-PVP	Laser Energy	800 mj/pulse
	No. pulses	1000 pulse
	Stock concentration	50 µg/mL
Zeta potential	-17.44 mV	
UV-vis (λ_{max} peaks)	1 day	402nm
	1 week	409nm
	2 week	410nm
TEM analysis	Avarege diameter	28.43nm

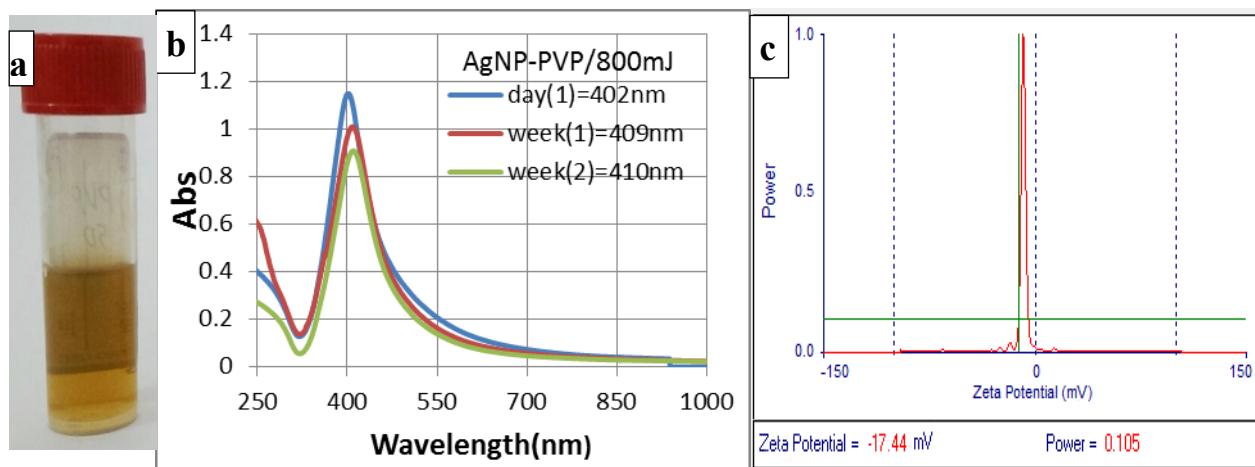


Figure 1: Characterization of synthesized AgNPs-PVP: (a) AgNPs-PVP colloidal; (b) UV-vis spectrum for three times; (c) Zeta potential analysis.

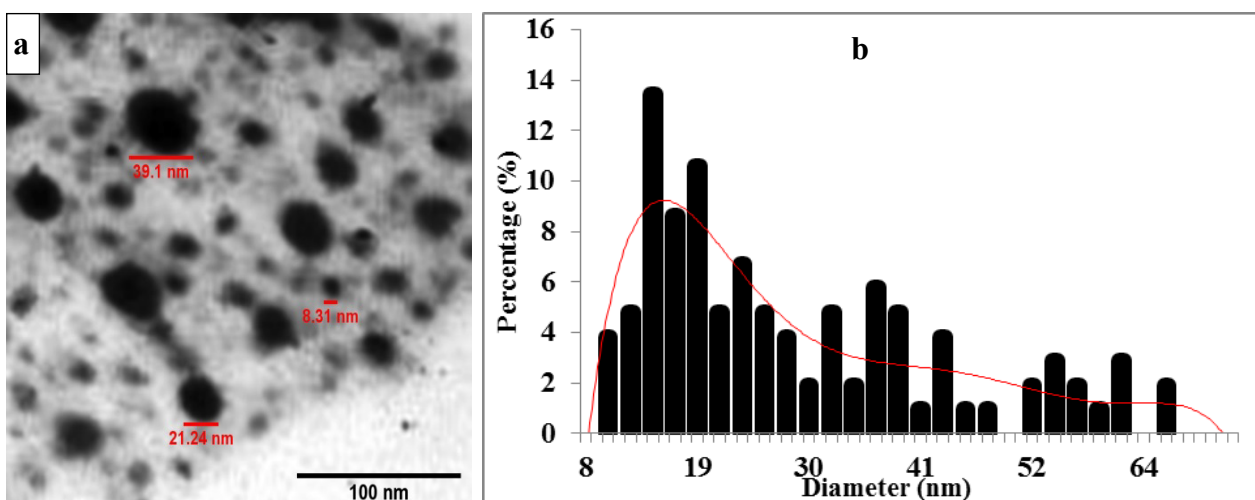


Figure 2: Size and morphology of AgNPs-PVP analysis by TEM. (a) Microphotographs were used to determine the size diameter and shape of nanoparticles. The average range of observed diameter was 28.43nm. (b) Particle size distributions from TEM microphotographs.

This absorbance peak indicated the spherical shape of the prepared AgNPs-PVP. Furthermore, the spectrum peak at this wavelength signify that the AgNPs in the (PVP) solution was spherical which confirmed by TEM results as shown in Fig 2a, b. The zeta potential values are provide convincing evidence that the particles have no tendency to agglomerate because the presence of charge on the surfaces of AgNPs which prevent agglomerate. The results showed that the synthesized AgNPs-PVP solution was (-17.44), is stable, table-1 and fig-1. The zeta value that obtained from this study for synthesized AgNPs-PVP corresponds to previous studies results (29, 30). As well, the UV-visible spectra of the AgNPs-PVP were measured after 1 and 2 weeks for same sample to investigate the ability of the PVP solution as a stabilizer. The absorption spectrum in, table

-1 and fig -1, show a marked reduction in absorbance peak in the old sample in comparison of fresh sample. Although, the spectrum peaks at these wavelengths did not deviated from 410nm after 2 weeks. The TEM micrographs shown are representative of the AgNP populations analyzed by Image-J software and offer the most accurate view of the particles' size and agglomeration. To determine their size accumulative distribution were used GETDATDW software, approximately measured more than 200 particles synthesized by pulse laser ablation from several samples and represented them as the size distribution analysis. Fig-2a, the TEM micrographs indicate to the spherical shape of AgNPs-PVP. The TEM micrographs for AgNPs-PVP analyzed revealed that the average size of the particles is (28.43 nm), the maximum diameter (65nm) and

minimum diameter (8.47nm). The largest proportion of particles ranging from (10-30nm). This type of NPs shape is suitable for drug loading and most biological applications (31).

Cytotoxicity and IC50

Cytotoxicity of AgNPs-PVP on HeLa, SKOV-3 cancer cell line and REF normal cell line via crystal violet assay showed that AgNPs-PVP were able to reduce viability of the HeLa, SKOV-3 and REF cells in a dose-dependent manner and exposure periods. The results revealed that AgNPs-PVP were high cytotoxic on cancer cells in comparison of normal cells during 24, 48, 72h exposure (fig-3a, b and c). The AgNPs possesses low toxicity to normal cells comparing with cancer cells, also is no significant difference between the 24 h and 48 h of cells exposure to AgNPs (32). The inhibited concentration IC50 of AgNPs-PVP into HeLa was 3.125µg/ml, while the IC50 of AgNPs-PVP into SKOV-3 was 12.5µg/ml, during 24hrs of exposure, which decreased the viability of cells to 50% comparing of the control. It is clear that the IC50 of the SKOV-3 cells is very higher than in Hela cells. Whereas, the inhibition rate of REF was very low comparing with the cancer cells and

IC50 of AgNPs-PVP did not appear during all three exposure periods. Therefore, the following tests were used on the IC50 values of HeLa and SKOV-3 cells. The finding of anticancer drugs that kills or disables tumor cells without undue toxicity on other cells are an extraordinary challenge (33). Particle size and zeta potential are important properties which may influence the biological activity of nanoparticles and has been suggested as a key factor through the interaction with charged surfaces. Nanoparticles with different particle sizes or zeta potential may have different mechanisms of inhibition (34). Sur et al. (35) indicated that lactose-modified AgNPs enter human lung cancer cells (A549) at a higher rate compared to their entrance into L929 fibroblasts. Similarly, human astrocytes (normal glial cell) were more resistant to PVP-coated AgNPs comparing to the lung cancer cells (36). Haase et al. (37) reported an IC50 value for peptide coated silver nanoparticles with a diameter of 20nm were 110 µg/mL. Priyadharshini et al. (38) reported that both AgNPs and ZnONPs did not show cytotoxicity against normal cell lines.

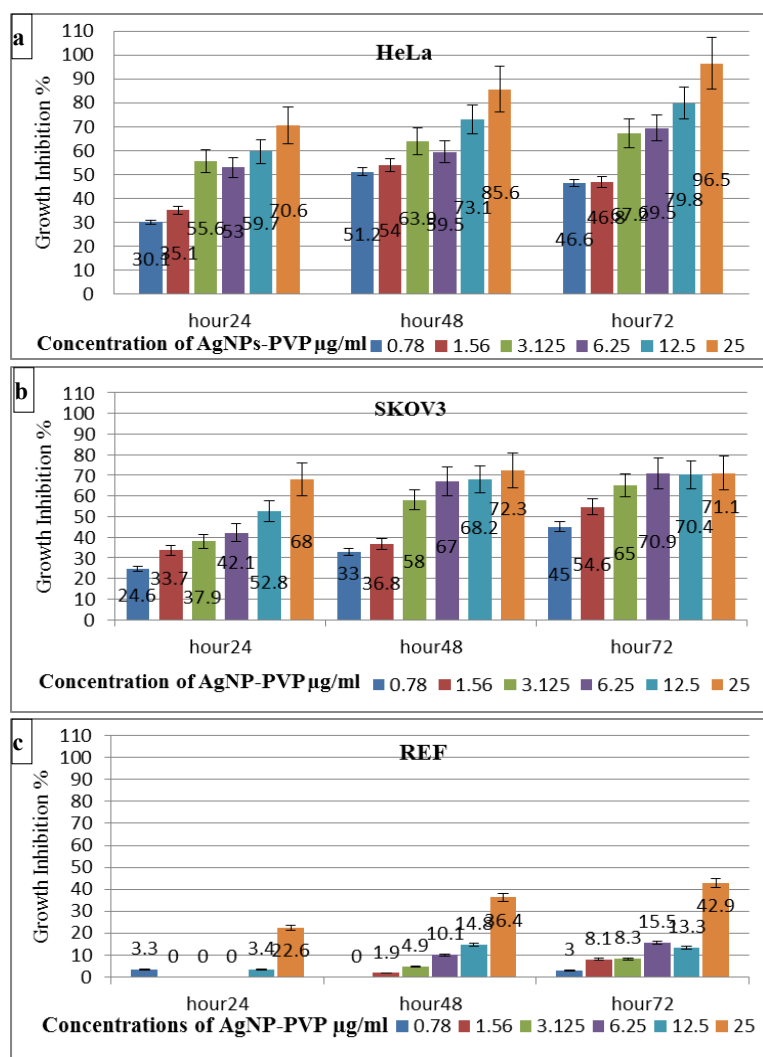


Figure (3): Cytotoxic of synthesized AgNPs-PVP at different concentrations and three times exposure on GI% rate for: (a) HeLa, (b) SKOV-3 and (c) REF cell lines.

In line with our results, many investigators showed that AgNPs induce *in vitro* cytotoxic responses often specific to cell types (39, 40, 23) resulting in varying degrees of toxicity and was depending on nanoparticle size, concentration and exposure time (41, 42). Other investigators endorsed the cytotoxicity of AgNPs to the oxidative stress caused by their release of Ag⁺ in cells as both silver nanoparticles and silver ions which could trigger the production of hydroxyl radicals in acidic endo/lysosomes (43). The growth inhibition rate dependent on the type of the cell line, exposure period and concentration, also in the nanoparticles experiments, the growth inhibition rate is also depending on size and shape of nanoparticles and surface chemistry etc. (44).

AgNPs induce mitochondrial-mediated apoptosis

Mitochondrial transmembrane potential (MTP) is an early event in apoptosis. MitoCapture monomer assay was used to evaluate the effect of AgNPs in mitochondrial membrane permeability. The results showed that the HeLa and SKOV-3 untreated cells were appearance of red fluorescence (red cells), while disappearance of red fluorescence and emergence of very strong green fluorescence was view in the HeLa and SKOV-3 treated cells with AgNPs-PVP IC₅₀, indicating that AgNPs-PVP could cause MTP collapse significantly higher in treated cells than untreated cells, fig-4. These results suggest that AgNPs could induce apoptosis through a mitochondria-mediated apoptosis pathway. AgNPs are known to induce cytotoxicity in several types of cancer cells by generation of

reactive oxygen species (ROS) and mitochondrial dysfunction and thus death cells (45). Mitochondria-mediated apoptosis undergoes two major changes which include changes in the permeabilization of the outer mitochondrial membrane and the loss of the electro chemical gradient (46). The permeabilization of the outer membrane is tightly regulated by a member of the Bcl-2 family. Membrane depolarization is mediated by the mitochondrial permeability transition pore. Prolonged mitochondrial permeability transition pore opening leads to a compromised outer mitochondrial membrane (46, 47). Mitochondria play important role in apoptosis, via the intrinsic apoptotic program. An intrinsic apoptotic pathway is the depolarization of the mitochondrial (mt) membrane. Depolarized mt is a result of the formation of mt permeability transition (PT) pores (48, 49). mt PT has been associated with various metabolic consequences such as halted functioning of the electron transport chain with associated elevation in ROS and decreased production of ATP (50). Govender et al. (48) observed a significant increase in mt depolarization after AgNPs treatment, with an accompanying decrease in ATP concentration. They concluded that the high levels of bax expression, high mt depolarization, and decreased ATP suggest that AgNPs induces cellular apoptosis in cancerous lung cells via the intrinsic apoptotic pathway. Several studies also suggested that nanoparticles seem to be localized in mitochondria and cause oxidative stress as well as potentiate structural damage and eventually lead to toxicity to the cells (51, 52, 53, 54).

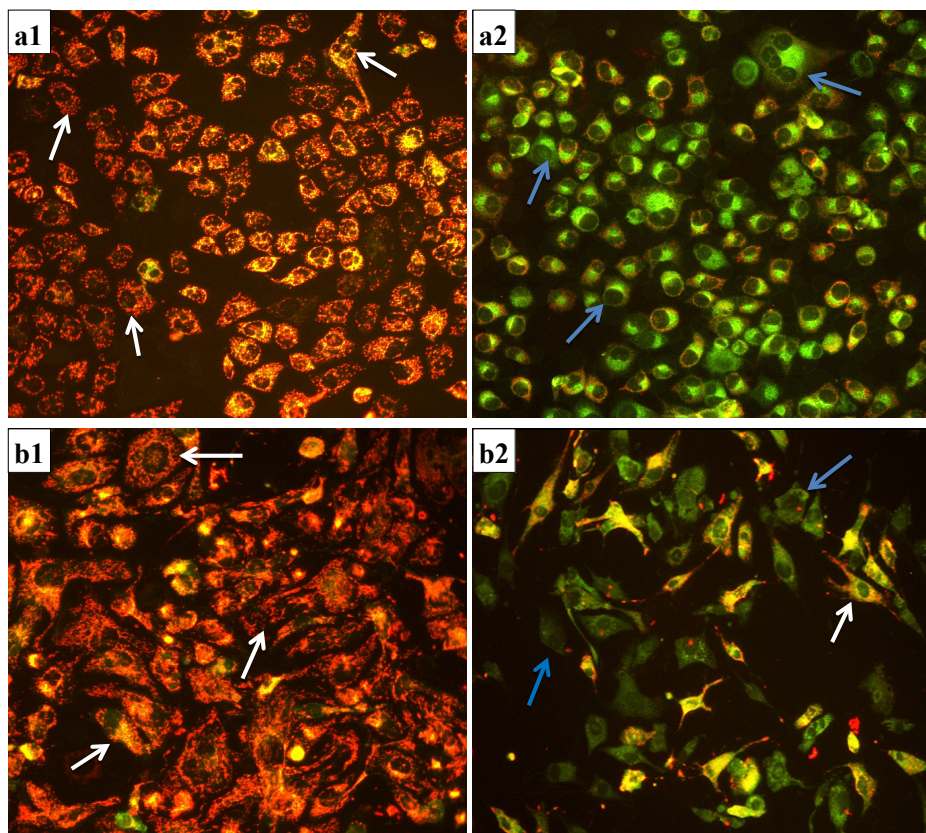


Figure (4): Microphotographs with a Leica inverted fluorescent microscope; Detection of Apoptosis in mitochondrial in cells that treated 24hrs with IC₅₀ of AgNPs-PVP: (a1) untreated HeLa (control); (a2) treated HeLa, (b1) untreated SKOV-3 (control); (b2) treated SKOV-3. Red cells viability (white arrow), green apoptotic cells (blue arrow).

Nuclear morphology of apoptosis

In this study, used the acridine orange/Propidium Iodide (AO/PI) double staining is well documented procedure to detect the apoptotic induced by IC50 synthesized AgNPs-PVP for each cell type. After exposure HeLa and SKOV-3 cancer cell lines with concentrations IC50 of AgNPs-PVP during 24hrs have shown to induce apoptosis in HeLa and SKOV-3 cells, when examined under fluorescent microscope (fig 5: a1,b1,c1and d1) using blue fluorescent filter and (fig 5 : a2, b2, c2 and d2) using green fluorescent filter. The results showed significant nuclear morphological changes in both cell type HeLa and SKOV-3 treated with AgNPs-PVP in comparison of untreated cells. The in vitro cytotoxic potential of AgNPs could attribute to the generation of ROS which have been shown to play an important role in induction of apoptosis (55) and induce membrane fluidity (56, 43). After the treatment with IC50 concentration of AgNPs, the induction of apoptosis was assessed for cancer cells by fluorescence microscopy stained with acridine orange/ethidium bromide (AO/EB). The acridine orange pen-

etrated the normal cell membrane and the cells were observed as green fluorescence; whereas in apoptotic cells and apoptotic bodies observed a nuclear shrinkage, nuclear damage and blebbing as orange colored bodies (57). These results indicate clearly that AgNPs-PVP induce apoptosis in all cancer cell lines trialed. The morphology of the necrotic, apoptotic, and normal cells were identified separately using fluorescence microscopy based on the cell membrane integrity. The nuclei of cancer cells treated with AgNPs were characterized by typical apoptotic hallmarks, clearly visible also in pictures. The ongoing apoptotic process started with the loss of nuclear shape and the expansion of nuclear material (58). Progressively, several nuclear apoptotic bodies containing the fragmented DNA were visible, appearing as green to yellow fluorescent patches (early apoptosis); in an advanced apoptotic stage the disintegration of apoptotic bodies lead to total nuclear DNA fragmentations typical of late apoptosis (orange to red stained nuclei). These confirm that apoptotic-like bodies are fundamental marks of apoptosis (59).

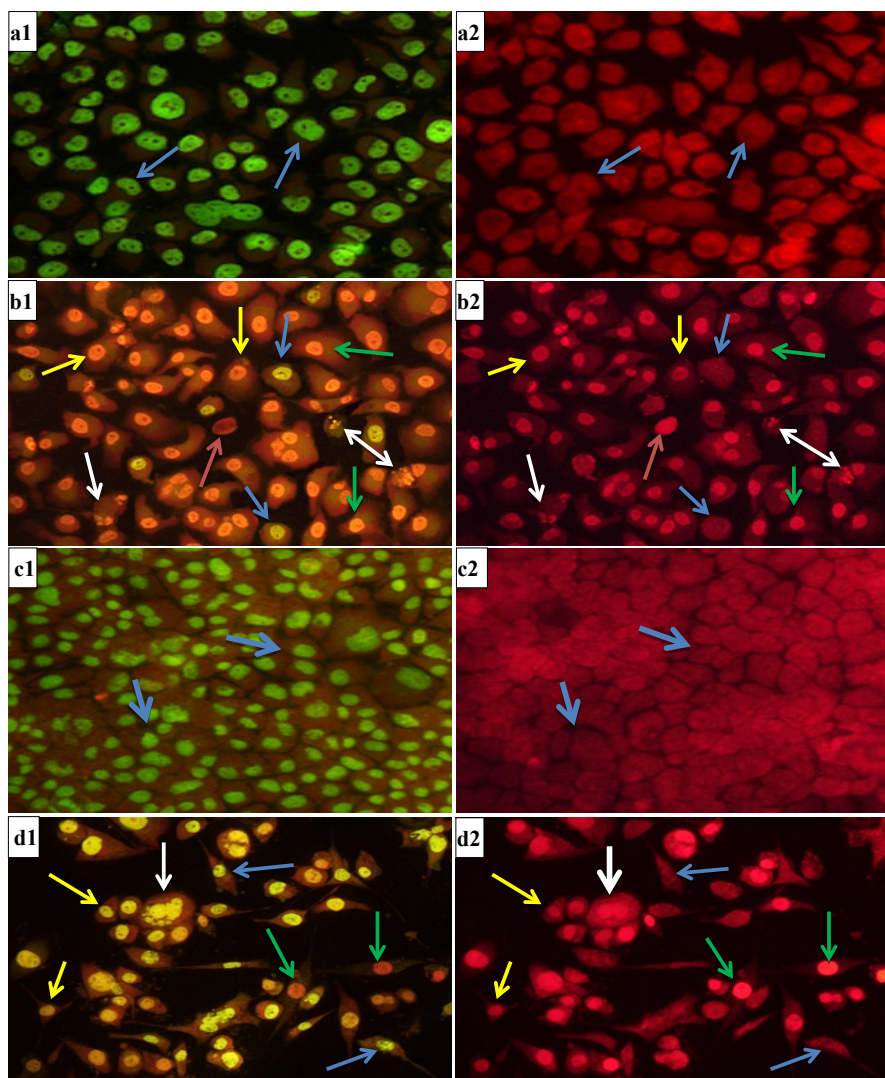
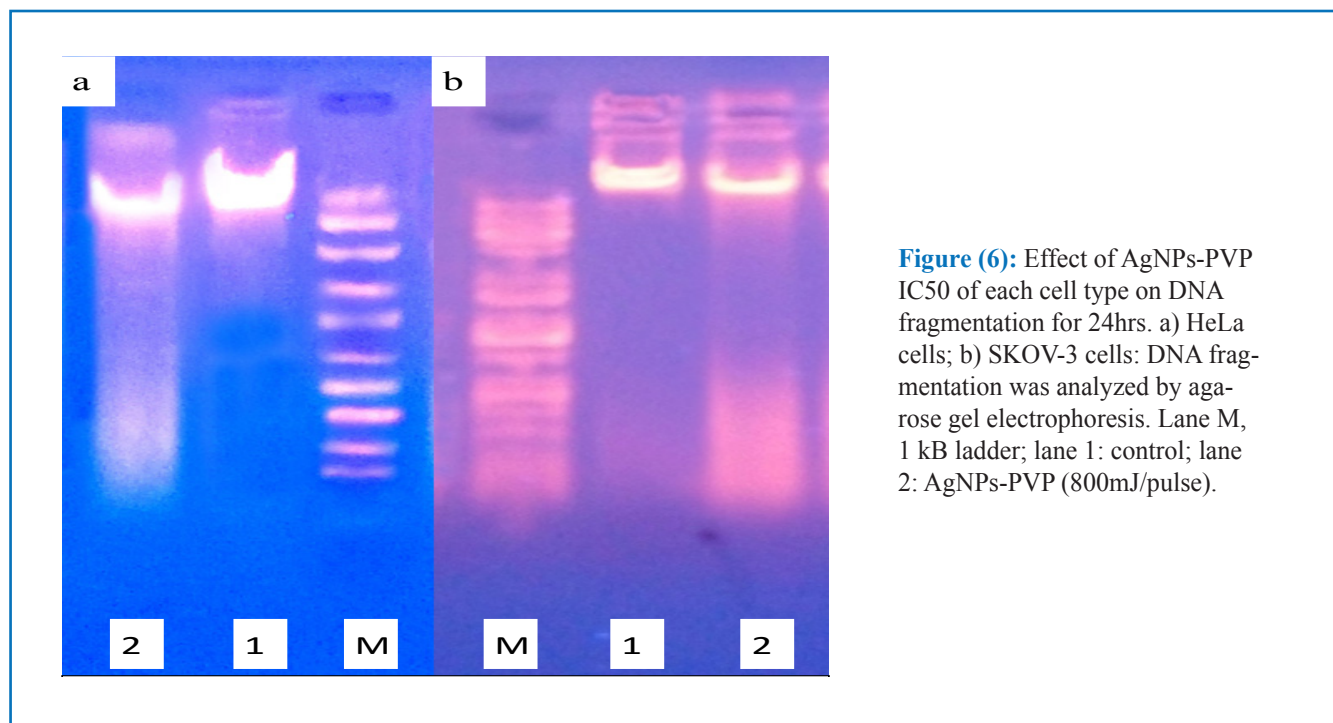


Figure (5): Detection of Apoptosis (AO/PI) in cells that treated with IC50 of AgNPs: (Lift image under blue fluorescent filter, Right image under green fluorescence filter). (a1, a2) untreated HeLa (control); (b1, b2) treated HeLa AgNPs-PVP; (c1, c2) untreated SKOV-3 (control); (b1, b2) treated SKOV-3 AgNPs-PVP. Blue arrow=living cells; yellow arrow=early apoptosis; green arrow=late apoptosis; white arrow= DNA fragment; red arrow= necrosis.

DNA fragmentation assay

Nucleosomal DNA fragmentation assay considers a biochemical hallmark of late apoptosis. Therefore, genomic DNA fragmentation assay was conducted to evaluate the ability of synthesized AgNPs-PVP IC50 by pulse laser ablation (at laser energy 800mJ/pulse), to induce DNA degradation of two cancer cell lines tested (HeLa and SKOV-3) for 24hrs of exposure. Agarose gel electrophoresis of genomic DNA treated with synthesized AgNPs IC50 for each cell type showed a smear like pattern (Fig-6). Treatment of AgNPs induced exacerbated apoptosis in the human ovarian cancer cells, which may cor-

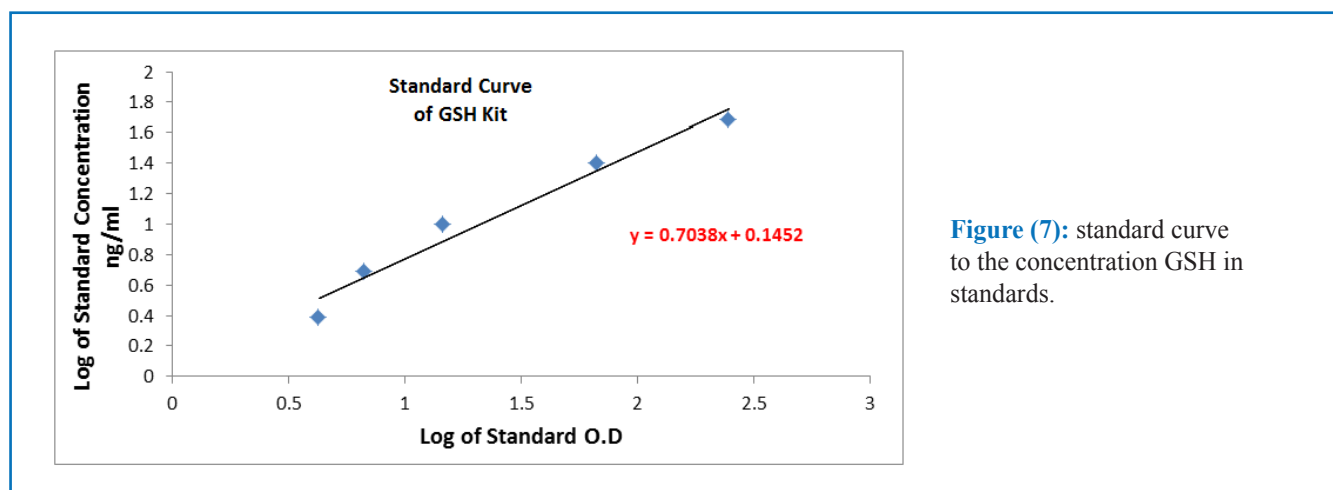
relate with alteration of cell morphology, enhanced Lactate dehydrogenase (LDH) release, reactive oxygen species (ROS) generation, oxidative stress, mitochondrial dysfunction, activation of caspase-3, and DNA fragmentation (45). Induction of apoptosis can be confirmed by two factors such as irregular reduction in size of cells, in which the cells are reduced and shrunken, and lastly DNA fragmentation (40). Gothandam and Balaji (60) reported that the silver nanoparticles exhibited significant cytotoxic effects and the apoptotic features were confirmed through caspase-3 activation and DNA fragmentation assays (61).



Effect of AgNPs synthesized on reduced glutathione (GSH) level in cytoplasm cells

To Verification of the effect of AgNPs on the GSH level, two cancer cell lines (HeLa and SKOV-3) were treated IC50 for synthesized AgNPs-PVP (at laser energy 800mJ/pulse) to esti-

mate GSH level in cell cytoplasm. A standard curve is plotted relating the intensity of the color (O.D.) to the concentration of the standards kit to extract the standard equation of the curve. The standard equation is used to determine the GSH concentration in each sample (fig -7).



The results showed that the level of GSH was slightly decreased after 24hrs treatment of synthesized AgNPs-PVP IC50 compared with of control (untreated cells) for HeLa and

SKOV-3 cancer cell lines with non-significant variation in GSH level (fig -8).

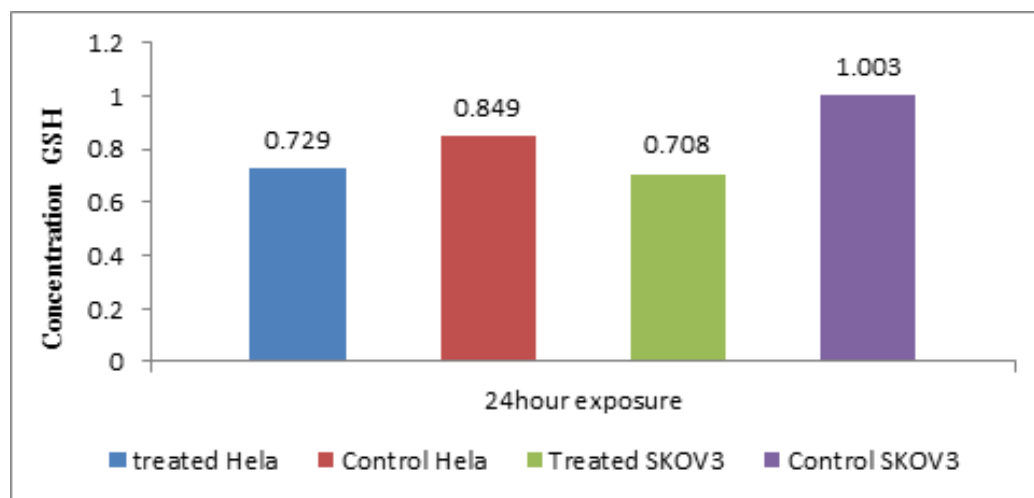


Figure (8): Levels of (GSH) in the cytoplasm of cancer cell lines exposed to AgNPs-PVP IC50.

Glutathione (GSH) is a tri-peptide antioxidant that plays a pivotal role in mitigating oxidative damage. GSH is oxidized by ROS to form a homodimer disulfide (GSSG) (62).

Intracellular reduced GSH scavenge ROS generated in cells to be oxidized to glutathione disulphide (GSSG). AgNO₃ penetrated the cell membrane and reacted with GSH, depleted its contents mostly due to oxidation of reduced GSH to GSSG 2 GSHGSSG+2H⁺ or likely that Ag²⁺ after penetration formed a silver–glutathione complex (63). The production of high levels of ROS molecules and hydrogen peroxide (H₂O₂) lead to cell death (64). Emphasized, Fahrenholtz, et. al. (30) during treatment A2780, SKOV-3, and OVCAR3 cells with PVP-coated AgNPs (10 and 100 µg/ml) for 24 h to quantify the cellular content of both oxidized (GSSG) and reduced glutathione (GSH) that the net effect of these cells were a decrease

in the GSH/GSSG ratio in SKOV-3 cells, but not in OVCAR3 and A2780 cells. The lack of correlation between the effects of AgNPs on GSH/GSSG and relative sensitivity of ovarian cancer cells to AgNPs exposure indicated that alteration of the GSH/GSSG ratio is unlikely to be the dominant mechanism by which AgNPs exert their cytotoxic effects. In the present study, we have successfully synthesized and prepared stable, spherical AgNPs-PVP with average sizes were 28.43nm, using laser device by pulse laser ablation at laser energy (800mJ/pulse) which is green, environmentally friendly, cost effective, and rapid method for synthesis of AgNPs. This study suggest that AgNPs-PVP have ability to inhibit the growth of cancer cells in different types of cancer cell lines, and the inhibition was different according to type of cell line with less effect on normal cells.

References:

- Kim, S-K. and Kalimuthu, S. (2014). Handbook of Anticancer Drugs from Marine Origin. (ed). Springer International Publishing Switzerland. 805pages.
- Morelli, V.; Zoorob, R. and Heidelbaugh, J.J. (2017). Primary Care of the Medically Underserved, An Issue of Primary Care: Clinics in Office Practice, E-Book. Volume 44, Issue 1 of The Clinics: Internal Medicine.
- Iraqi Cancer Board. (2015). Results of the Iraqi Cancer Registry 2012. Baghdad, Iraq, Iraqi Cancer Registry Center, Ministry of Health, 2015.
- Alwan N.A.S. (2016). Breast Cancer among Iraqi women: Preliminary Findings from a Regional Comparative Breast Cancer Research Project. Journal of Global Oncology, ASCO, 2 (1): 1-4.
- World Health Organization. (2014). "Cancer Fact Sheet N°297". Chapter 5.12. ISBN 9283204298.
- National cancer institute (2017). Types of cancer treatment. The national institutes of health.
- Mishra, J.; Dromund, J.; Quazi, S.H.; Karanki, S.S.; Shaw, J.J.; Chen, B. and Kumar, N. (2013). Prospective of Colon Cancer Treatments and Scope for Combinatorial Approach to Enhanced Cancer Cell Apoptosis. Crit Rev Oncol Hematol. 86(3): 232–250.
- Nikalje AP (2015) Nanotechnology and its Applications in Medicine. Med chem 5(2): 081-089.
- Alshahrani, A. (2016). The Advantages of Nanotechnology in Medical Field. IJIREICE, 4(4): 4401 - 4405.
- de Moraes, M.G.; Martins, V.G.; Steffens, D.; Pranke, P. and Cos-

- ta, J. A.V. (2014). Biological Applications of Nanobiotechnology. *Journal of Nanoscience and Nanotechnology*. Vol. 14, 1007–1017.
11. Hasan, S. (2015). A Review on Nanoparticles: Their Synthesis and Types. *Research Journal of Recent Sciences*. 4(), 9-11.
 12. Hackenberg S, Scherzed A, Kessler M, Froelich K, Ginzkey C, Koehler C, Burghartz M, Hagen R, Kleinsasser N (2010). Zinc oxide nanoparticles induce photocatalytic cell death in human head and neck squamous cell carcinoma cell lines in vitro. *Int J Oncol* 37: 1583–1590.
 13. Elangovan K, Elumalai D, Anupriya S, Shenbagaraman R, Kaleena PK, Murugesan K. (2015). Phyto mediated biogenic synthesis of silver nanoparticles using leaf extract of *Andrographis echinoides* and its bio-efficacy on anticancer and antibacterial activities. *J Photochem Photobio B Biol*. 151:118–124.
 14. Lee, S.M.; Kim, D.; Jeon, D.Y. and Choi, K.C. (2012). Nanoplasmon-Enhanced Transparent Plasma Display Devices. *Small*, 8(9): 1350–1354.
 15. Chen, X.; Jia, B. H.; Saha, J. K.; Cai, B. Y.; Stokes, N.; Qiao, Q.; Wang, Y. Q.; Shi, Z. R. and Gu, M. (2012). "Broadband enhancement in thin film amorphous silicon solar cells enabled by nucleated silver nanoparticles," *Nano Lett*. 12, 2187–2192.
 16. Xiping, L.; Shengli, L.; Miaotao, Z.; Wenlong, Z. and Huanghong, L. (2011). Evaluations of antibacterial activity and cytotoxicity on Ag nanoparticles. *Rare Metal Materials. Engin*. 40 : 209–214.
 17. Singh, R.P. and Ramarao, P. (2012). Cellular uptake, intracellular trafficking, and cytotoxicity of silver nanoparticles. *Toxicol Lett*, 213: 249–259.
 18. Tajdidzadeh, M.; Zakaria, A.B.; Z. Abidin Talib, Z.; Gene, A.S. and Shirzadi, S. (2017). Optical Nonlinear Properties of Gold Nanoparticles Synthesized by Laser Ablation in Polymer Solution. *Journal of Nanomaterials*. 2017(12): 1-9.
 19. Garcia-Guillena, G.; Mendivil-Palmaa, M.I.; Krishnana, B.; Avelanada, D.; Castilloa, G.A.; DasRoya, T.K. and Shajia, S. (2015). Structure and morphologies of ZnO nanoparticles synthesized by pulsed laser ablation in liquid: Effects of temperature and energy fluence. *Materials Chemistry and Physics*. 162: 561-570.
 20. Tawfeeq, A.T.; Kadhim, H.M.; Yaseen, N.Y.; Kalil, S.K.; Ghedan, A.F. Hussein, R.A. and Abdul-Lateaf, A.Y. (2015). Genotoxicity of Silver Nanoparticles synthesized by Laser Ablation Method in Vivo. *Iraqi Journal of Cancer and Medical Genetics* 8 (1): 21-30.
 21. Yang, S. Cai, W. Liu, G. and Zeng, H. (2009). From Nanoparticles to Nanoplates: Preferential Oriented Connection of Ag Colloids during Electrophoretic Deposition. *J. Phys. Chem. C* 113: 7692–7696.
 22. Sanpui, P.; Chattopadhyay, A. and Ghosh, S.S. (2011). Induction of apoptosis in cancer cells at low silver nanoparticle concentrations using chitosan nanocarrier. *ACS Appl Mater Interfaces*. 3(2):218–228.
 23. Jeyaraj, M.; Sathishkumar, G.; Sivanandhan, G.; Ali, D. M.; Rajesh, M.; Arun, R.; Kapildev, G.; Manickavasagam, M.; Thajuddin, N.; Premkumar, K. and Ganapathi, A. (2013a). Biogenic silver nanoparticles for cancer treatment: An experimental report. *Colloids and Surfaces B: Biointerfaces*. 106: 86–92.
 24. Parnsamut, C. and Brimson, S. (2015). Effects of silver nanoparticles and gold nanoparticles on IL-2, IL-6, and TNF- α production via MAPK pathway in leukemic cell lines. *Genet. Mol. Res*. 14 (2): 3650-3668.
 25. Elshawy, O.E.; Eman A. Helmy, E.A. and Rashed, L.A. (2016). Preparation, Characterization and in Vitro Evaluation of the Antitumor Activity of the Biologically Synthesized Silver Nanoparticles. *Advances in Nanoparticles*, 5, 149-166.
 26. SAS. (2012). Statistical Analysis System, User's Guide. Statistical. Version 9.1th ed. SAS. Inst. Inc. Cary. N.C. USA.
 27. Tajdidzadeh, M.; Azmi, B.Z.; Mahmood, W.; Yunus, M.; Abidin Talib, Z.; Sadrolhosseini, A.R.; Karimzadeh, K.; Gene, S.A. and Dorraj, M. (2014). Synthesis of Silver Nanoparticles Dispersed in Various Aqueous Media Using Laser Ablation. *The ScientificWorld Journal*. Volume 2014 (2014), Article ID 324921, 7 pages.
 28. Zamiri, R.; Azmi, B.Z.; Sadrolhosseini, A.R.; Ahangar, H.A.; Zaidan, A.W. and M. A. Mahdi, M.A. (2011). Preparation of silver nanoparticles in virgin coconut oil using laser ablation. *International Journal of Nanomedicine*. 6(1): 71–75.
 29. El-Sonbaty, S. M. (2013). Fungus-mediated synthesis of silver nanoparticles and evaluation of antitumor activity. *Cancer Nano* 4:73–79.
 30. Fahrenheitoltz, C.D.; Swanner, J.; Ramirez-Perez, M. and Singh, R. N. (2017). Heterogeneous Responses of Ovarian Cancer Cells to Silver Nanoparticles as a Single Agent and in Combination with Cisplatin. *Journal of Nanomaterials*. 2017(7353):1-11.
 31. Khanna, P.K. and Nair, C. K. K. (2009). Synthesis of silver nanoparticles using cod liver oil (fish oil): green approach to nanotechnology. *International Journal of Green Nanotechnology: Physics and Chemistry*, 1: 3–9.
 32. Shahbazzadeh D.; Ahari H. A. A.; Anvar A. A.; Moaddab S.; Asadi T.; Shokrgozar M. A. and Rahman-Nya J. (2011). In vitro effect of Nanosilver toxicity on fibroblast and mesenchymal stem cell lines. *Iranian Journal of Fisheries Sciences*, 10(3): 487-496.
 33. Hameed, S. V.; Sultana, J.; Ara, S.; Ehteshamul-Haque, and Athar, M. (2009). Toxicity of *Fusarium solani* strains on brine shrimp (*Artemia salina*). *Zoological Research*, 30, 468–472.
 34. Bihari P, Vippola M, Schultes S, Praetner M, Khandoga A, Reichel C et al (2008) Optimized dispersion of nanoparticles for biological in vitro and in vivo studies. *Part Fiber Toxicol* 5:14
 35. Sur, I.; Cam, D.; Kahraman, M.; Baysal, A. and Culha, M. (2010). Interaction of multi-functional silver nanoparticles with living cells.
 36. Luther, E.M., Koehler, Y., Diendorf, J., Epple, M., Dringen, R., 2011. Accumulation of silver nanoparticles by cultured primary brain astrocytes. *Nanotechnology* 22, 375101.
 37. Haase, A., Rott, S., Manton, A., Graf, P., Plendl, J., Thünemann, A.F., Meier, W.P., Taubert, A., Luch, A., Reiser, G., 2012. Effects of silver nanoparticles on primary mixed neural cell cultures: uptake, oxidative stress and acute calcium responses. *Toxicol. Sci*. 126, 457–468.
 38. Priyadharshini, R. I.; Prasannaraj, G.; Geetha, N. and Venkatachalam, P. (2014). Microwave-Mediated Extracellular Synthesis of Metallic Silver and Zinc Oxide Nanoparticles Using Macro-Algae (*Gracilaria edulis*) Extracts and Its Anticancer Activity Against Human PC3 Cell Lines. *Appl Biochem Biotechnol*, 174: 2777–2790.
 39. Zhang, X.F., Choi, Y.J., Han, J.W., Kim, E., Park, J.H., Gurunathan, S. and Kim, J.H. (2015) Differential Nanoreprotoxicity of Silver Nanoparticles in Male Somatic Cells and Spermatogonial Stem Cells. *International Journal of Nanomedicine*, 10, 1335-1357.
 40. Gurunathan, S., Han, J.W., Eppakayala, V., Jeyaraj, M. and Kim, J.H. (2013) Cytotoxicity of Biologically Synthesized Silver Nanoparticles in MDA-MB-231 Human Breast Cancer Cells. *BioMed Research International*, 2013, Article ID: 535796.
 41. Park, S., Lee, Y.K., Jung, M., Kim, K.H., Chung, N., et al. (2007) Cellular Toxicity of Various Inhalable Metal NanoO. particles on Human Alveolar Epithelial Cells. *Inhalation Toxicology: International Forum for Respiratory*, 19, 59-65.
 42. Hess, L.K., Jones, L., Schlager, J.J., et al. (2008) Unique Cellular Interaction of Silver Nanoparticles: Size-Dependent Generation of Reactive Oxygen Species. *Journal of Physical Chemistry B*, 112, 13608-13619.
 43. Foldbjerg, R., Olesen, P., Hougaard, M., Dang, D.A., Hoffmann, H.J. and Autrup, H. (2009) PVP-Coated Silver Nanoparticles and Silver Ions Induce Reactive Oxygen Species, Apoptosis and Necrosis in THP-1 Monocytes. *Toxicology Letters*, 190, 156-162.

44. Qu, X.; Yao, C.; Wang, J.; Li, Z. and Zhang, Z. (2012). AntiCD30-targeted gold nanoparticles for photothermal therapy of L-428 Hodgkin's cell Int J Nanomedicine, 7: 6095-6103.
45. Zhang, X. and Gurunathan, S. (2016). Combination of salinomycin and silver nanoparticles enhances apoptosis and autophagy in human ovarian cancer cells: an effective anticancer therapy. International Journal of Nanomedicine, 11: 3655–3675.
46. Kimata M, Matoba S, Iwai-Kanai E, Nakamura H, Hoshino A, Nakaoka M, et al. p53 and TIGAR regulate cardiac myocyte energy homeostasis under hypoxic stress. Am J Physiology-Heart Circulatory Physiology. 2010;299:H1908–16.
47. Rasola A, Bernardi P. The mitochondrial permeability transition pore and its involvement in cell death and in disease pathogenesis. Apoptosis. 2007;12:815–33.
48. Govender R, Phulukdaree A, Gengan RM, Anand K, Chuturgoon AA. Silver nanoparticles of Albizia adianthifolia: the induction of apoptosis in human lung carcinoma cell line. J Nanobiotechnology. 2013;11:5.
49. Hirsch T, Marzo I, Kroemer G. Role of the mitochondrial permeability transition pore in apoptosis. Biosci Rep. 1997;17:67–76.
50. Wang X. The expanding role of mitochondria in apoptosis. Genes Dev. 2001;15:2922–33.
51. Carlson C, Hussain SM, Schrand AM, Braydich-Stolle LK, Hess KL, Jones RL, et al. Unique cellular interaction of silver nanoparticles: size-dependent generation of reactive oxygen species. J Physical Chem B. 2008;112:13608–19.
52. Xia T, Kovochich M, Liang M, Madler L, Gilbert B, Shi H, et al. Comparison of the mechanism of toxicity of zinc oxide and cerium oxide nanoparticles based on dissolution and oxidative stress properties. ACS Nano. 2008;2:2121–34.
53. Xia T, Kovochich M, Brant J, Hotze M, Sempf J, Oberley T, et al. Comparison of the abilities of ambient and manufactured nanoparticles to induce cellular toxicity according to an oxidative stress paradigm. Nano Lett. 2006;6:1794–807.
54. Derfus AM, Chan WCW, Bhatia SN. Intracellular delivery of quantum dots for live cell labeling and organelle tracking. Adv Mater. 2004;16:961–+.
55. Liu, W., Wu, Y., Wang, C., Li, H.C., Wang, T., Liao, C.Y., Cui, L., Zhou, Q.F., Yan, B. and Jiang, G.B. (2010) Impact of Silver Nanoparticles on Human Cells Effect of Particle Size. Nanotoxicology, 4, 319-330.
56. AshaRani, P.V., Hande, M.P. and Valiyaveetil, S. (2009) Anti-Proliferative Activity of Silver Nanoparticles. BMC Cell Biology, 10, 65.
57. Ashokan, A. P.; Paulpandi, M.; Dinesh, D.; Murugan, K.; Vadivalagan, C. and Benelli, G. (2016). Toxicity on Dengue Mosquito Vectors Through Myristica fragrans-Synthesized Zinc Oxide Nanorods, and Their Cytotoxic Effects on Liver Cancer Cells (HepG2). Journal of Cluster Science, 28(1): 205–226.
58. Mandelkow, R. Gumbel, D. Ahrend, H. Kaul, A. Zimmermann, U. Burchardt, M. And Matthias B. Stope, M.B. (2017). Detection and Quantification of Nuclear Morphology Changes in Apoptotic Cells by Fluorescence Microscopy and Subsequent Analysis of Visualized Fluorescent Signals. Anticancer Research 37: 2239-2244.
59. D'Archivio, M., Santangelo, C., Scazzocchio, B., Vari, R., Filesi, C., Masella, R. and Giovannini, C. (2008). Modulatory effects of polyphenols on apoptosis induction: Relevance for cancer prevention. International Journal of Molecular Science 9: 213-228.
60. Gothandam, K. M. and Balaji, K. (2016). Cytotoxic Effect on Cancerous Cell Lines by Biologically Synthesized Silver Nanoparticles. Braz. Arch. Biol. Technol. 59: e16150529.
61. Gurunathan, S.; Raman, J.; Abd Malek, N.; AJohn, P. and Viki-neswary, S. (2013b). Green synthesis of silver nanoparticles using Ganoderma neo-japonicum Imazeki: a potential cytotoxic agent against breast cancer cells. International Journal of Nanomedicine 8: 4399–4413.
62. Wu, J.H. and Batist, G. (2013). Glutathione and glutathione analogues; therapeutic potentials. Biochim Biophys Acta. 1830(5):3350–3353.
63. Khan H, Khan MF, Asim-ur-Rehman, Jan SU, Ullah N. (2011). The protective role of glutathione in silver induced toxicity in blood components. Pak J Pharm Sci 24(2):123–128.
64. Kim DW, Hong GH, Lee HH, Choi SH, Chun BG, Won CK, Hwang IK, Won MH. (2007). Effect of colloidal silver against the cytotoxicity of hydrogen peroxide and naphthazarin on primary cultured cortical astrocytes. Neuroscience 117(3):387–400.

استخدام جسيمات الفضة النانوية المصنعة بطريقة الاستئصال النبضي الليزري في محلول *polyvinylpyrrolidone* في تثبيط النمو وحث الموت المبرمج في نوعين من خطوط الخلايا السرطانية النسائية

نوفل ناظم الراوي¹، محمد قيس العاني¹، عامر طالب توفيق²، ناهي يوسف ياسين²

1 علوم الحياة/ كلية العلوم/ جامعة الأنبار

2 المركز العراقي لحوث السرطان والوراثة الطبية/ الجامعة المستنصرية

الخلاصة:

صنعت جسيمات فضة نانوية مغلقة بمادة (PVP) بطريقة فيزيائية من خلال الازالة بالليزر النبضي وبطاقة (800) ملي جول/نبضة. تم توصيف جسيمات الفضة المصنعة باستخدام مطياف الأشعة فوق البنفسجية وقياس جهد الزيتا وتم قياس تركيز الجسيمات داخل المحلول المحضر بواسطة طيف الامتصاص الذري. كما تم توصيف شكل وحجم جسيمات الفضة المصنعة باستخدام المجهر الالكتروني. جرى مقارنة تأثير جسيمات الفضة النانوية على نوعين من خطوط السرطانية (سرطان عنق الرحم وسرطان المبيض) مع خط الخلايا الطبيعي (خلايا جنين الفأر). اظهرت النتائج بأن متوسط حجم جسيمات الفضة النانوية المصنعة كانت (28,43 nm) وذات شكل كروي تقريبا، كما اظهرت رنين بلازمون سطحي يتراوح بين (402-410nm). وان التركيز الكلي لجسيمات الفضة المصنعة كانت (50 µg/m). عولمت الخلايا بعدة تراكيز متدرجة لجسيمات الفضة النانوية (0,78 و 1,56 و 3,125 و 6,25 و 12 و 25 µg/ml) وبفترات حضان (24 و 48 و 72 ساعة). بينت فحوصات السمية ان جسيمات الفضة المصنعة بمادة (PVP) لها تأثير تثبيطي عالي على كل من خلايا سرطان الرحم والمبيض اعتمادا على التركيز والوقت، بينما اظهرت مستوى تثبيطي واطى على خلايا الفأر الطبيعية. تم تحديد التركيز المثبط النصفى (IC 50) خلال 24 ساعة من التعرض في كل من خلايا سرطان الرحم والمبيض (3,75 µg/ml و 12,5 µg/ml) على التوالي، بينما لم يكن هناك مستوى تثبيطي نصفى على خلايا الفأر الطبيعية. اختبرت سمية التركيز المثبط النصفى (IC 50) على كل من خلايا سرطان الرحم والمبيض. وقد اظهرت النتائج بان جسيمات الفضة النانوية المصنعة قد حثت على حدوث الموت المبرمج في المايتوكوندريا وفي انوية الخلايا وكذلك حدوث تقطع في مادة الخلايا الوراثية DNA، بينما لم يتغير مستوى GSH كثيرا مقارنة بخلايا السيطرة (الغير معاملة). تشير هذه النتائج الى امكانية استخدام جسيمات الفضة المصنعة والمغلقة بمادة (PVP) في علاج انواع مختلفة من السرطانات.